PV based Isolated DC-DC Converter Fed Induction Motor Drive Applications

R Venkata Krishna, V L Surya Prabha, A Pradeep Kumar

Assoc. Professor & HOD, Department of EEE, LORDS Inst. of Engg. & Tech, JNTUH, India

Asst. Professor, Department of EEE, LORDS Inst. of Engg. & Tech, JNTUH, India

M. Tech Scholar, Department of EEE, LORDS Inst. of Engg. & Tech, JNTUH, India

ABSTRACT: The dual active bridge (DAB) topology as an attractive alternative to full-bridge topology. In comparison with the conventional full bridge topology, the output inductor is transferred to the ac side, and is in series with the leakage inductance. Consequently, the energy in the leakage inductance is transferred to the load without causing reverse recovery losses in the output diodes. This allows higher switching frequencies and, therefore, an increase in power density. In this project three-phase dual active bridge (DAB) topology used as high-power-density dc–dc converter for railway applications. The three-phase DAB is analyzed concerning the current intervals, the output power, and soft switching region, including the impact of zero-voltage switching capacitors. Furthermore, two measures are proposed to achieve soft-switching in the entire operating range, being auxiliary inductors and a straightforward switching strategy called the burst mode. Optimal component values are calculated to minimize losses in the complete operating range and to assess which measure is best suited. The proposed with topologic is RES and Induction Motor drive system .The simulation results are presented by using Matlab/Simulink software.

KEYWORDS: DC–DC power conversion, power electronics, power supplies, rail transportation electronics.

I. INTRODUCTION

Solar energy is the most low cost, competition free, universal source of energy as sun shines throughout. This energy can be converted into useful electrical energy using photovoltaic technology. The steady state reduction of price per peak watt and simplicity with which the installed power can be increased by adding panels are attractive features of PV technology. Among the many applications of PV energy, pumping is the most promising. In a PV pump storage system, solar energy is stored, when sunlight is available as potential energy in water reservoir and consumed according to demand. There are advantages in avoiding the use of large banks of lead acid batteries, which are heavy and expensive and have one fifth of the lifetime of a PV panel. A number of simulation DC motor driven PV pumps are already in use in several parts of the world, but they suffer from maintenance problems due to the presence of the commutator and brushes. Hence a pumping system based on an induction motor can be an attractive proposal where reliability and maintenance-free operations with less cost are important. The effective operation of Induction motor is based on the choice of suitable converter-inverter system that is fed to Induction Motor.

For PV applications like pumping these converters could do a good job as pumping is carried out at high power. Thus a new push pull converter which is two switch topology can do justice by giving a high power throughout. The Induction Motors are the AC motors and hence from converter, an inverter system is also required to obtain an AC voltage. This inverter is chosen based on its advantages and it is fed to induction motor.

Photovoltaic technology is one of the most promising for distributed low-power electrical generation. The steady reduction of price per peak watt over recent years and the simplicity with which the installed power can be increased by adding panels are some of its attractive features. Among the many applications of photovoltaic energy, pumping is one of the most promising. In a photovoltaic pump-storage system, solar energy is stored, when sunlight is available, as potential energy in a water reservoir and then consumed according to demand. There are advantages in avoiding the use

of large banks of lead-acid batteries, which are heavy and expensive and have one-fifth of the lifetime of a photovoltaic panel. It is important, however, that the absence of batteries does not compromise the efficiency of the end-to-end power conversion chain, from panels to mechanical pump. Photovoltaic panels require specific control techniques to ensure operation at their maximum power point (MPP). Impedance matching issues mean that photovoltaic arrays may operate more or less efficiently, depending on their series/parallel configuration.

II. TOPOLOGY OVERVIEW

The field of high-power-density dc–dc converters has been addressed often in the last decades. From the beginning, the conventional full-bridge converter topology has been the preferred choice to realize a high-power dc–dc converter [1].However, due to problems with the leakage inductance of the transformer and, consequently, reverse recovery losses of the output diodes, the maximum switching frequency is limited. To solve this problem, several solutions were presented, including active clamps and/or auxiliary circuits [2]–[4]. These solutions enable higher switching frequencies at the expense of additional components and could lead to higher device stress. The additional components impede the increase in power density and increased complexity, while the efficiency is often not better compared to other zero-voltage switching (ZVS) and zero-current switching (ZCS) techniques. Resonant converter topologies offer possibilities for ZVS or ZCS, enabling high efficiencies and power densities [5]–[7]. The series resonant or LLC converter provides a load independent operating point with unity voltage gain at a switching frequency near the resonance frequency [6], [8]–[10]. However, this load independent operating point is lost when the input and/or output voltage changes, and switching frequency control is necessary to regulate the output voltage. Therefore, a boost converter can be used to regulate the input voltage in order to guarantee operation in the load independent operating point [10], [11]. Alternatively, the resonance circuit can be influenced by a switch-controlled capacitor, resulting in fixed frequency operation [12]. Despite the provided solutions, the LLC converter still suffers from high rms phase currents, requiring a relatively large series resonant capacitor that leads to a decreased power density. The additional boost converter or switch-controlled capacitor also deteriorates the power density and efficiency.

The dual active bridge (DAB) topology introduced in [1]is an attractive alternative to the problems with the classical full-bridge topology. In comparison with the conventional full bridge topology, the output inductor is transferred to the ac side, and is in series with the leakage inductance. Consequently, the energy in the leakage inductance is transferred to the load without causing reverse recovery losses in the output diodes. This allows higher switching frequencies and, therefore, an increase in power density. Furthermore, the use of an active output bridge also increases the power density of the transformer [1]. When the desired inductance can be incorporated in the transformer, again the power density can be increased. In [13], very high power densities, up to 11.13kW/L, are reported. A three-phase DAB, also proposed in [1], has some advantages in comparison to the single-phase DAB. The three-phase DAB has lower turn-off currents in the switches and lower rms currents per phase. Also, the VA ratings for the input and output filters are significantly lower and can even go to zero due to the three-phase characteristics. Besides the lower VA ratings, the effective ripple frequency of the filter currents is three times higher, allowing to use smaller filters. Compared to the single-phase DAB, the currents through the transformer windings are much more sinusoidal, resulting in reduced high frequency losses in the transformers [14]. A comprehensive comparison of single-phase and three-phase DAB topologies is given in [1].Both the single-phase and three-phase DAB topologies suffer from a limited soft-switching range in case the input voltage and the reflected output voltage are not equal. For the single-phase DAB, there exist switching strategies or modulation schemes for increasing the soft-switching range. These are described. Here, the soft-switching operating range is increased and also the overall efficiency can be increased with a minimum loss modulation strategy. The three-phase DAB does not possess these advantageous switching possibilities. The phase shift angle φ between the bridge voltage is the only control variable as the symmetrical properties of the three-phase system have to be maintained [14].Although the three-phase DAB has less switching possibilities, compared to the single-phase DAB, and includes four extra switches, the topology has the most preferred properties for designing a high-power density isolated dc–dc converter. It has the lowest component ratings and is capable of achieving higher output powers with possibly the highest power density. For APU applications in light rail vehicles, high-power capability and power density are decisive. Therefore, the three phase DAB topology is selected in this study.

III. THREE-PHASE DAB DC–DC CONVERTER

The three-phase DAB, shown in Fig. 1(a), consists of two three-phase bridges coupled with a three-phase transformer connected in Y–Y. The bridges are operated in six-step mode at a constant frequency. By applying a phase shift between the input and Output Bridge, the power flow can be controlled. Because the converter is symmetrical from input to output, bidirectional power flow is possible. The transformer leakage inductances are used as current transfer elements and, therefore, not considered as parasitic. If the magnetizing inductance Lm is neglected, an equivalent circuit can be used for analysis. In this circuit, only the total leakage inductance Ls seen from the primary side is connected between the phase legs from the input and output bridge. The corresponding idealized waveforms are shown in Fig. 1(b).

A. Analysis

To analyze the soft-switching region, the current of phase A is defined for the first six intervals as depicted in Fig. 1(b). The current iA in the different intervals is given in (3) for phase shifts of $0 \leq \varphi \leq \pi3$. For phase shifts of $\pi3 \leq \varphi \leq 23\pi$, a second set of equations, not given here, is utilized for further analysis of the soft-switching region. The magnetizing inductance Lm of the transformer is neglected in the analysis. Furthermore, the angular frequency is defined as $\omega = 2\pi fs$, with fs the switching frequency in Hertz. The transformer's leakage inductance is indicated with Ls and the input and output voltages are defined as Vi and Vo, respectively. The reflected output voltage is given by Vo= VoN, with N the turns ratio of the transformer. Because the phase current is symmetric, the current iA(0) can be found by solving the set of equations, assuming steady-state
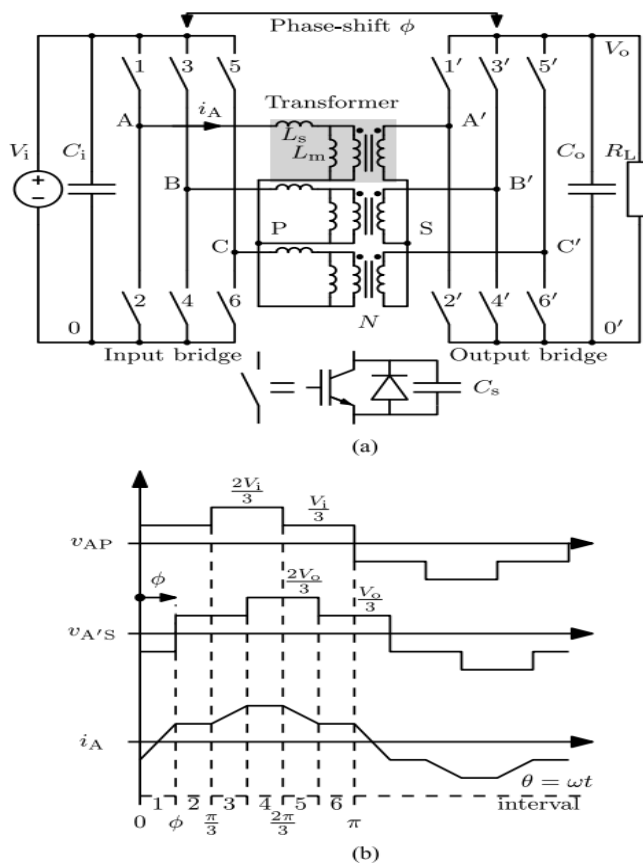

Fig.1. Three-phase DAB. (a) Topology. (b) Idealized waveforms, gating signals can be found in [1].

Condition iA(0) = −iA(π). This results in

$$i_A(0) = \frac{1}{3\omega L_s}\left[\frac{2\pi}{3}(V_o' - V_i) - V_o'\phi\right] \tag{1}$$

B. Output Power

Under the assumption of a lossless converter, the output power Po can be found with

$$P_o = P_i = \frac{3}{\pi}\int_0^\pi v_{AP}(\theta)i_A(\theta)d\theta \tag{2}$$

$$i_A(\theta) = \begin{cases} i_A(0) + \frac{V_i + V_o'}{3\omega L_s}\theta & \forall\ 0 \le \theta \le \phi & :\text{interval 1} \\ i_A(\phi) + \frac{V_i - V_o'}{3\omega L_s}(\theta - \phi) & \forall\ \phi \le \theta \le \frac{\pi}{3} & :\text{interval 2} \\ i_A(\frac{\pi}{3}) + \frac{2V_i - V_o'}{3\omega L_s}(\theta - \frac{\pi}{3}) & \forall\ \frac{\pi}{3} \le \theta \le \frac{\pi}{3} + \phi & :\text{interval 3} \\ i_A(\frac{\pi}{3} + \phi) + \frac{2V_i - 2V_o'}{3\omega L_s}(\theta - \frac{\pi}{3} - \phi) & \forall\ \frac{\pi}{3} + \phi \le \theta \le \frac{2\pi}{3} & :\text{interval 4} \\ i_A(\frac{2\pi}{3}) + \frac{V_i - 2V_o'}{3\omega L_s}(\theta - \frac{2\pi}{3}) & \forall\ \frac{2\pi}{3} \le \theta \le \frac{2\pi}{3} + \phi & :\text{interval 5} \\ i_A(\frac{2\pi}{3} + \phi) + \frac{V_i - V_o'}{3\omega L_s}(\theta - \frac{2\pi}{3} - \phi) & \forall\ \frac{2\pi}{3} + \phi \le \theta \le \pi & :\text{interval 6} \end{cases} \tag{3}$$

Finally, the expression of the output power for $0 \le \varphi \le 23\pi$ is

$$P_o = \begin{cases} \frac{V_i V_o'}{\omega L_s}\phi\left[\frac{2}{3} - \frac{\phi}{2\pi}\right] & \text{for } 0 \le \phi \le \frac{\pi}{3} \\ \frac{V_i V_o'}{\omega L_s}\left[\phi - \frac{\phi^2}{\pi} - \frac{\pi}{18}\right] & \text{for } \frac{\pi}{3} \le \phi \le \frac{2\pi}{3} \end{cases} \tag{4}$$

C. Soft-Switching Region

Minimizing the switching losses is the key to achieve a high switching frequency. The turn-on losses are of main interest because excessive losses in the switch and the anti parallel diode can arise when the anti parallel diodes experience the reverse recovery process. The input bridge faces this problem when iA(0) > 0. Therefore, the current has to fulfill iA(0) ≤ 0 to ensure soft-switching in the input bridge. During the switching transient, the current iA is considered constant. Rewriting (1)to the required constraint gives the phase shift for ensuring soft turn-on of the switches in the input bridge, this is found to be

$$\phi_i \ge \frac{2\pi(V_o' - V_i)}{3V_o'} \tag{5}$$

A similar derivation can be made for the output bridge, where the output bridge is soft-switching for iA(φ) ≥ 0. Using (3) and(1) gives the required phase shift to ensure soft turn-on of the switches in the output bridge, resulting in

$$\phi_o \ge \frac{2\pi(V_i - V_o')}{3V_i} \tag{6}$$

1) Impact of ZVS Capacitors: ZVS capacitors, or snubber capacitors, are used to reduce turn-off losses. These are connected in parallel to the switches and supplement the output capacitance, as can be seen in Fig. 1(a). After a switch turns OFF, there is a small blanking time tb before the opposite switch of the same leg turns on. During tb, the current commutates to the ZVS capacitors and divides equally over the two capacitors of the phase leg. In this transition, one capacitor is charged while the other is discharged. This implies that the load current must be high enough to enable a full charge or discharge of the ZVS capacitors for a given tb. Assuming a constant current during the switching transient, the soft-switching constraint for enabling of turn-on of the switches in the input bridge is changed to

$$i_{\mathrm{A}}(0) + \frac{2C_{\mathrm{s}}V_i}{t_{\mathrm{b}}} \leq 0 \tag{7}$$

and for the output bridge to

$$i_{\mathrm{A}}(\phi) - \frac{2C_{\mathrm{s}}V_{\mathrm{o}}}{t_{\mathrm{b}}N} \geq 0 \tag{8}$$

Where C_s represents a ZVS capacitor connected in parallel to the switch, and t_b is a fixed blanking time. A more accurate, current depending charge-based ZVS analysis is reported. However, to investigate the impact of the ZVS capacitors and approximate the soft-switching region, the presented current based method is sufficient. Solving (7) and (8) for the phase-shift φ gives the soft switching region for the input bridge and the output bridge, respectively. These are given by

$$\phi_{\mathrm{i}} \geq \frac{2\pi_i(V_{\mathrm{o}}' - V_{\mathrm{i}})}{3V_{\mathrm{o}}'} + \frac{2C_{\mathrm{s}}V_{\mathrm{i}}}{V_{\mathrm{o}}'t_{\mathrm{b}}}3\omega L_{\mathrm{s}} \tag{9}$$

$$\phi_{\mathrm{o}} \geq \frac{2\pi(V_{\mathrm{i}} - V_{\mathrm{o}}')}{3V_{\mathrm{i}}} + \frac{2C_{\mathrm{s}}V_{\mathrm{o}}}{V_{\mathrm{i}}t_{\mathrm{b}}N}3\omega L_{\mathrm{s}} \tag{10}$$

D. Extension of the Soft-Switching Region

Auxiliary power converters for railway applications have to be able to operate from no-load to full-load conditions over the whole input voltage range. This means that the converter has to operate outside the soft-switching region. Therefore, two methods to extend the soft-switching operation of the converter have been investigated.

1) Auxiliary Inductors: The first method is based on adding reactive currents to fully charge or discharge the ZVS capacitors during the switching transient. The reactive currents are injected with three star-connected auxiliary inductors per bridge. This has the same effect as the magnetizing inductances of the transformers, which are also connected in star. However, separate auxiliary inductors are preferred to have more design flexibility. The peak current, injected by the auxiliary inductors during the switching transient, is calculated from the voltage waveforms shown in Fig. 1(b). For the input bridge, the peak current is calculated as

$$\hat{i}_{\mathrm{a-i}} = \frac{2\pi V_{\mathrm{i}}}{9\omega L_{\mathrm{a-i}}} \tag{11}$$

and for the output bridge as

$$\hat{i}_{\mathrm{a-o}} = \frac{2\pi V_{\mathrm{o}}}{9\omega L_{\mathrm{a-o}}N} \tag{12}$$

Next, the soft-switching constraints from (7) and (8) can be extended to

$$i_{\mathrm{A}}(0) + \frac{2C_{\mathrm{s}}V_{\mathrm{i}}}{t_{\mathrm{b}}} - \frac{2\pi V_{\mathrm{i}}}{9\omega L_{\mathrm{a-i}}} \leq 0 \tag{13}$$

and for the output bridge to

$$i_{\mathrm{A}}(\phi) - \frac{2C_{\mathrm{s}}V_{\mathrm{o}}}{t_{\mathrm{b}}N} + \frac{2\pi V_{\mathrm{o}}}{9\omega L_{\mathrm{a-o}}N} \geq 0 \tag{14}$$

Then, the soft-switching region can be calculated with the minimum phase shift for the input bridge

$$\phi_i \geq \frac{2\pi(V_o' - V_i)}{3V_o'} + \frac{2C_s V_i}{V_o' t_b}3\omega L_s - \frac{2\pi V_i L_s}{3V_o' L_{a-i}} \quad (15)$$

and for the output bridge

$$\phi_o \geq \frac{2\pi(V_i - V_o')}{3V_i} + \frac{2C_s V_o}{V_i t_b N}3\omega L_s - \frac{2\pi V_o L_s}{3V_i L_{a-o}N} \quad (16)$$

As shown with (15) and (16), the auxiliary inductance decreases the required phase-shift for operating in a soft-switching manner. To achieve soft-switching in the whole operating range,(15) and (16) should be solved for zero phase-shift, i.e., no-load condition. The corresponding values. For relatively low- and high-input voltages, the required values for La−i and La−o are low and, therefore, also causing high reactive currents. The use of auxiliary inductors presents a clear disadvantage due to the reduced efficiency and power density.

2) Burst Mode: The second method does not use any extra components but relies on a straightforward switching strategy. When the required output power Po is lower than the minimum load for soft switching, the converter switches from continuous mode to burst mode. In the burst mode, the converter operates with an output power Pb high enough to enable soft-switching .An example of the burst mode with the corresponding waveforms is shown in Fig. 2(a). The average output power is defined as

$$< p_o > = \frac{n}{m}P_b, \qquad \forall \quad 1 \leq n \leq m \quad (17)$$

Where n is the amount of switching cycles operating with po =Pb and m is the total amount of switching cycles of one burst cycle. The value of Pb depends on the soft-switching region of the converter. When nTs < t ≤ mTs, the output power po = 0 W, thus the output capacitor delivers the required current to the load, introducing a small voltage ripple. The output voltage ripple can be calculated with

$$\Delta v_o = \frac{I_o \Delta t}{C_o} \quad (18)$$

Where Io =<po >Vo=nPbmVo and Δt = m−nfs . This results in

$$\Delta v_o = \frac{n(m - n)P_b}{mV_o C_o f_s} \quad (19)$$

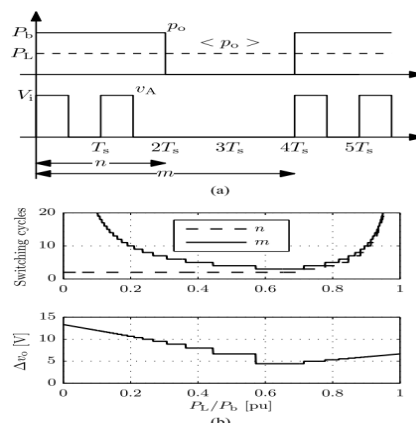An example of the output voltage ripple with n ≥ 2 is shown in Fig. 2(b).

Fig. 2. Burst-mode waveforms. (a) Burst-mode definitions. (b) Output voltage ripple with n ≥ 2, Pb = 80 kW, Vo = 600 V, Co = 1 mF, and fs = 20 kHz.

The downside of this method is the need for a larger output capacitance for the same voltage ripple requirements in normal operation without the burst mode. Furthermore, while the switching frequency is unchanged, the converter becomes audible due to the discontinuous operation.

IV. PHOTOVOLTAIC SYSTEM AND INDUCTION MOTOR (IM)

A Photovoltaic (PV) system directly converts solar energy into electrical energy. The basic device of a PV system is the PV cell. Cells may be grouped to form arrays. The voltage and current available at the terminals of a PV device may directly feed small loads such as lighting systems and DC motors or connect to a grid by using proper energy conversion devices this photovoltaic system consists of three main parts which are PV module, balance of system and load. The major balance of system components in this systems are charger, battery and inverter.
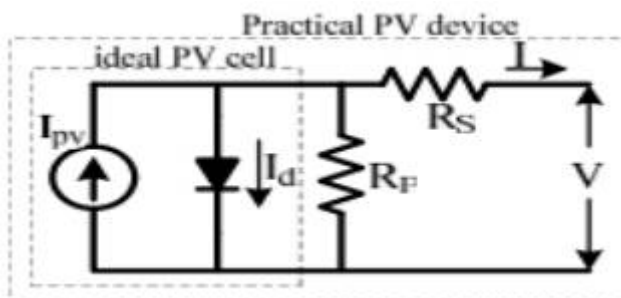
. Practical PV device.

A photovoltaic cell is basically a semiconductor diode whose p–n junction is exposed to light. Photovoltaic cells are made of several types of semiconductors using different manufacturing processes. The incidence of light on the cell generates charge carriers that originate an electric current if the cell is short circuited1
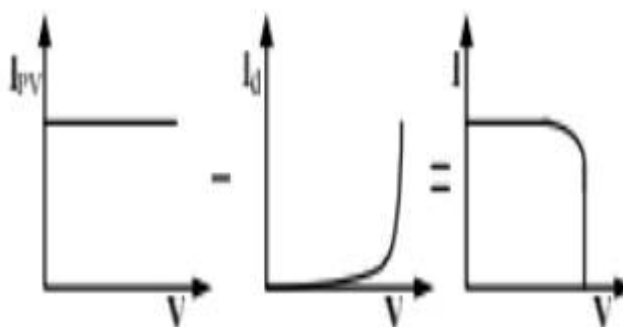
. Characteristics I-V curve of the PV cell.

The equivalent circuit of PV cell In the above figure the PV cell is represented by a current source in parallel with diode. Rs and Rp represent series and parallel resistance respectively.
The output current and voltage form PV cell are represented by I and V. The I-Characteristics of PV cell are shown in fig.6. The net cell current I is composed of the light generated current IPV and the diode current ID

INDUCTION MOTOR (IM)

An induction motor is an example of asynchronous AC machine, which consists of a stator and a rotor. This motor is widely used because of its strong features and reasonable cost. A sinusoidal voltage is applied to the stator, in the induction motor, which results in an induced electromagnetic field. A current in the rotor is induced due to this field, which creates another field that tries to align with the stator field, causing the rotor to spin. A slip is created between these fields, when a load is applied to the motor. Compared to the synchronous speed, the rotor speed decreases, at

higher slip values. The frequency of the stator voltage controls the synchronous speed. The frequency of the voltage is applied to the stator through power electronic devices, which allows the control of the speed of the motor. The research is using techniques, which implement a constant voltage to frequency ratio. Finally, the torque begins to fall when the motor reaches the synchronous speed. Thus, induction motor synchronous speed is defined by following equation,

$$n_s = \frac{120f}{P}$$

Where f is the frequency of AC supply, n, is the speed of rotor; p is the number of poles per phase of the motor. By varying the frequency of control circuit through AC supply, the rotor speed will change.

A. Control Strategy of Induction Motor

Power electronics interface such as three-phase SPWM inverter using constant closed loop Volts l Hertz control scheme is used to control the motor. According to the desired output speed, the amplitude and frequency of the reference (sinusoidal) signals will change. In order to maintain constant magnetic flux in the motor, the ratio of the voltage amplitude to voltage frequency will be kept constant. Hence a closed loop Proportional Integral (PI) controller is implemented to regulate the motor speed to the desired set point. The closed loop speed control is characterized by the measurement of the actual motor speed, which is compared to the reference speed while the error signal is generated. The magnitude and polarity of the error signal correspond to the difference between the actual and required speed. The PI controller generates the corrected motor stator frequency to compensate for the error, based on the speed error.
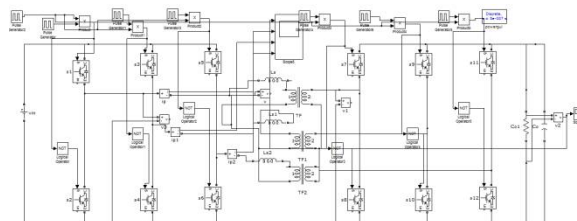
V.MATLAB/SIMULATION RESULTS

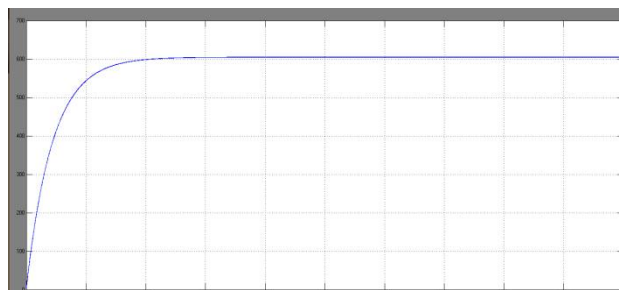Fig 3 Matlab/simulation conventional circuit of three-phase DAB dc-dc converter Topology.

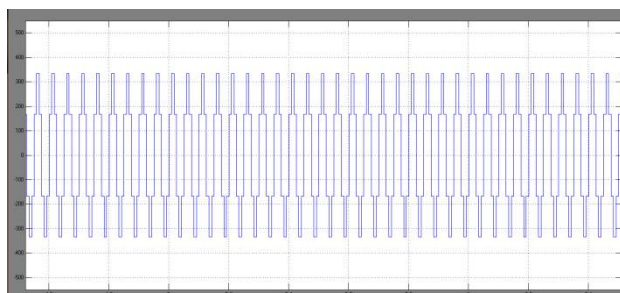Fig 4 simulation wave form of output voltage

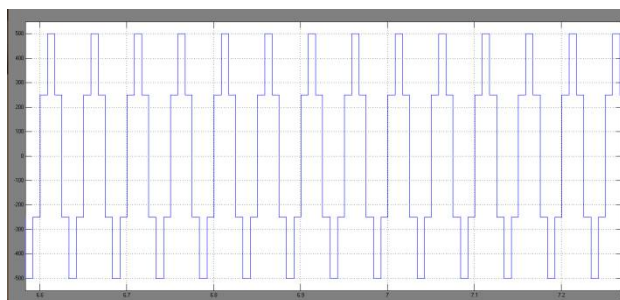Fig 5 simulation wave form of input line voltage at 750v

Fig 6 simulation wave form of input line voltage at 750 v

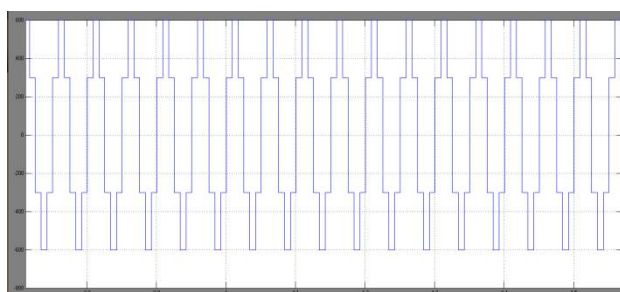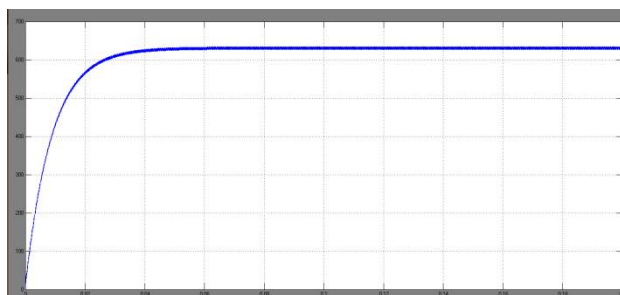Fig 7 simulation wave form of input line voltage at 900v
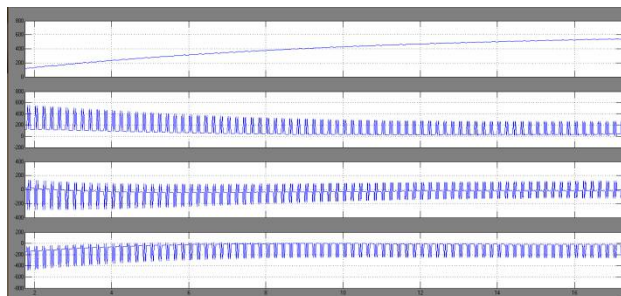

Fig 8 simulation wave form of output voltage

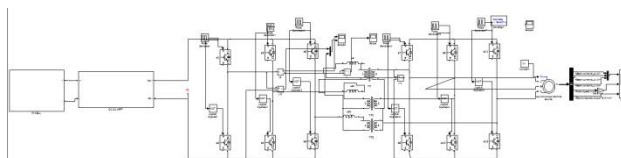Fig 9 simulation wave form of line voltages and currents

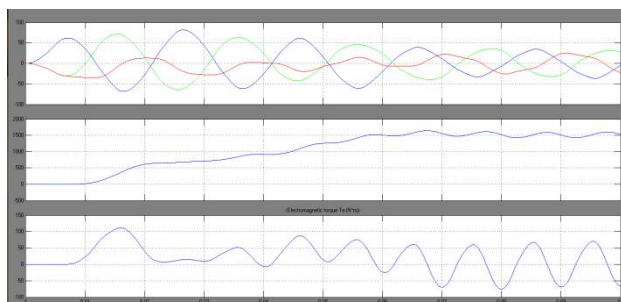Fig 10 Matlab/simulation proposed method of three-phase DAB dc-dc converter Topology with Induction Motor

Fig 11 simulation wave form of dc-dc converter Topology with Induction Motor torque, speed and voltage

VI.CONCLUSION

This work has evaluated the strategy for utilization of PV Cells for induction motor pumping. The electricity bill gets reduced since solar energy is utilized for agriculture pumping. The Photo Voltaic powered three phase induction motor drive system is successfully designed, modeled and simulated using Matlab/Simulink. The concept of Photo Voltaic pumping is proposed. The simulation results of three phase induction motor for Photo Voltaic pumping are presented. The simulation results are in line with the theoretical results. The scope of this work is the simulation and implementation of three phase PV Powered Induction motor drive system.

REFERENCES

[1].Nico H. Baars, Student Member, IEEE, Jordi Everts, Member, IEEE, Henk Huisman, Jorge L. Duarte, Member, IEEE, and Elena A. Lomonova, Senior Member, IEEE"A 80-kW Isolated DC–DC Converter m for Railway Applications"IEEE Transactions On Power Electronics, Vol. 30, No. 12, December 2015.
[2] R. De Doncker, D. Divan, and M. Kheraluwala, "A three-phase softswitched high-power-density dc/dc converter for high-power applications," IEEE Trans. Ind. Appl., vol. 27, no. 1, pp. 63–73, Jan. 1991.
[3] J. Dudrik, P. Spanik, and N.-D. Trip, "Zero-voltage and zero-current switching full-bridge dc-dc converter with auxiliary transformer," IEEE Trans. Power Electron., vol. 21, no. 5, pp. 1328–1335, Sep. 2006.
[4] J.-G. Cho, C.-Y. Jeong, and F. Lee, "Zero-voltage and zero-currentswitching full-bridge PWM converter using secondary active clamp," IEEE Trans. Power Electron., vol. 13, no. 4, pp. 601–607, Jul. 1998.
[5] O. Patterson and D. Divan, "Pseudo-resonant full bridge dc/dc converter," IEEE Trans. Power Electron., vol. 6, no. 4, pp. 671–678, Oct. 1991.
[6] R. Steigerwald, "A comparison of half-bridge resonant converter topologies," IEEE Trans. Power Electron., vol. 3, no. 2, pp. 174–182, Apr. 1988.
[7] A. Bhat and R. Zheng, "Analysis and design of a three-phase LCC-type resonant converter," IEEE Trans. Aerospace and Electron. Syst., vol. 34, no. 2, pp. 508–519, Apr. 1998.
[8] R. Steigerwald, "High-frequency resonant transistor dc-dc converters," IEEE Trans. Ind. Electron., vol. IE-31, no. 2, pp. 181–191, May 1984.

[9] X. Li, "A LLC-type dual-bridge resonant converter: Analysis, design, simulation, and experimental results," IEEE Trans. Power Electron., vol. 29, no. 8, pp. 4313–4321, Aug. 2014.

[10] J.-W. Kim and G.-W. Moon, "A new LLC series resonant converter with a narrow switching frequency variation and reduced conduction losses," IEEE Trans. Power Electron., vol. 29, no. 8, pp. 4278–4287, Aug. 2014.

[11] S. De Simone, C. Adragna, C. Spini, and G. Gattavari, "Design-oriented steady-state analysis of LLC resonant converters based on FHA," in Proc. Int. Symp. Power Electron., Electr. Drives, Autom. Motion,, May 2006, pp. 200–207.

[12] B.-C. Kim, K.-B. Park, C.-E. Kim, B.-H. Lee, and G.-W. Moon, "LLC resonant converter with adaptive link-voltage variation for a high-powerdensity adapter," IEEE Trans. Power Electron., vol. 25, no. 9, pp. 2248– 2252, Sep. 2010.

[13] Z. Hu, Y. Qiu, L. Wang, and Y.-F. Liu, "An interleaved LLC resonant converter operating at constant switching frequency," IEEE Trans. Power Electron., vol. 29, no. 6, pp. 2931–2943, Jun. 2014.

[14] M. Pavlovsky, S. de Haan, and J. Ferreira, "Reaching high power density in multikilowatt dc-dc converters with galvanic isolation," IEEE Trans. Power Electron., vol. 24, no. 3, pp. 603–612, Mar. 2009.

BIOGRAPHY

Mr. **R.Venkata Krishna** Graduated from Sree Kavitha Engineering College, Khammam, Andhra Pradesh in the year 2007, .M.Tech from Mahaveer institute of science & technology, Hyderabad in the year 2009. He is presently working as Assoc. Professor & Head in the Department of Electrical and Electronics Engineering, Lords Institute of Engineering & Tech. Himayithsagar, Hyderabad, India. His research areas include Electrical Power Systems and Electrical Drives..

Mrs. V L Surya Prabha, is Graduated from JITM, Parlakimundi, Orrisa, in the year 2004, M.Tech from Vitam, Vishakapatnam, Andhrapradesh in the year 2015. She is presently working as Assistant Professor in the Department of Electrical and Electronics Engineering, Lords Inst of Engg. & Tech., Himayat sagar, Hyderabad, Telangana, India. Her research areas include Power Systems & Instrument Transformers.

Mr. A Pradeep Kumar, is a PG student of Specilization power Electronics in the dept of Electrical and Electronics Engineering, Lords Inst of Engg. & Tech., Himayatsagar, Hyderabad, Telangana, India. He is pursuing his project study in the area of power Electronics and Drives.